



# Combined Radiomics–Clinical Model to Predict Radiotherapy Response in Inoperable Stage III and IV Non-Small-Cell Lung Cancer

Technology in Cancer Research & Treatment  
Volume 21: 1–13  
© The Author(s) 2022  
Article reuse guidelines:  
sagepub.com/journals-permissions  
DOI: 10.1177/15330338221142400  
journals.sagepub.com/home/tct  


Wenrui Chen, MS<sup>1,\*</sup>, Li Wang, PhD<sup>1,\*</sup>, Yu Hou, MS<sup>1</sup>, Lan Li, MS<sup>1</sup>, Li Chang, PhD<sup>1</sup>, Yunfen Li, PhD<sup>1</sup>, Kun Xie, MS<sup>2</sup>, Linbo Qiu, BS<sup>1</sup>, Dan Mao, BS<sup>1</sup>, Wenhui Li, PhD<sup>1</sup> , and Yaoxiong Xia, PhD<sup>1</sup>

## Abstract

**Purpose:** Radiotherapy is a promising treatment option for lung cancer, but patients' responses vary. The purpose of the study was to investigate the potential of radiomics and clinical signature for predicting the radiotherapy sensitivity and overall survival of inoperable stage III and IV non-small-cell lung cancer (NSCLC) patients. **Materials:** This retrospective study collected 104 inoperable stage III and IV NSCLC patients at the Yunnan Cancer Hospital from October 2016 to September 2020. They were divided into radiation-sensitive and non-sensitive groups. We used analysis of variance (ANOVA) to select features and support vector machine (SVM) to build the radiomic model. Furthermore, the logistic regression method was used to screen out clinically relevant predictive factors and construct the combined model of radiomics–clinical features. Finally, survival was estimated using the Kaplan–Meier method. **Results:** There were 40 patients in the radiation-sensitive group and 64 in the non-sensitive group. These patients were divided into training set (73 cases) and testing set (31 cases) according to the ratio of 7:3. Nine radiomics features and one clinical feature were significantly associated with radiotherapy sensitivity. Both the radiomics model and combined model have good predictive performance (the areas under the curve (AUC) values of the testing set were 0.864 (95% confidence interval [CI]: 0.683–0.996) and 0.868 (95% CI: 0.689–1.000), respectively). Only platelet level status was associated with overall survival. **Conclusion:** The combined model constructed based on radiomics and clinical features can effectively identify the radiation-sensitive population and provide valuable clinical information. Patients with higher platelet levels may have a poor prognosis.

## Keywords

radiomics signature, computed tomography, lung neoplasms, radiosensitivity, prognosis factors

## Abbreviations

AE, auto-encoder; ANOVA, analysis of variance; AUC, areas under the curve; CEA, carcinoembryonic antigen; CECT, contrast-enhanced computed tomography; CI, confidence interval; CR, complete response; CT, computed tomography; DCA, decision curve analysis; EGFR, epidermal growth factor receptor; EGFR-TKI, epidermal growth factor receptor–tyrosine kinase inhibitor; HU, housefield units; IMRT, intensity-modulated radiation therapy; KRAS, Kirsten rat sarcoma viral oncogene; KW,

<sup>1</sup> Department of Radiation Oncology, The Third Affiliated Hospital of Kunming Medical University, Yunnan Cancer Hospital, Kunming, Yunnan, China

<sup>2</sup> Department of Radiology, The Third Affiliated Hospital of Kunming Medical University, Yunnan Cancer Hospital, Kunming, Yunnan, China

\*These authors wish it be known that they contributed equally to this study and should be regarded as joint first authors.

## Corresponding Authors:

Wenhui Li, PhD, Department of Radiation Oncology, The Third Affiliated Hospital of Kunming Medical University, Yunnan Cancer Hospital, 519 Kunzhou Rd., Kunming, Yunnan 650118, China.  
Email: wenhuili64@yeah.net

Yaoxiong Xia, PhD, Department of Radiation Oncology, The Third Affiliated Hospital of Kunming Medical University, Yunnan Cancer Hospital, 519 Kunzhou Rd., Kunming, Yunnan 650118, China.  
Email: 55490850@qq.com



Kruskal–Wallis; LDA, linear discriminant analysis; LR-Lasso, logistic regression-least absolute shrinkage and selection operator; NLR, neutrophil-to-lymphocyte ratio; NPV, negative predictive value; NSCLC, non-small-cell lung cancer; OS, overall survival; PD, progressive disease; PPV, positive predictive value; PR, partial response; Rad-Score, radiomics score; RECIST, response evaluation criteria in solid tumors; RFE, recursive feature elimination; ROC, receiver operating characteristic; ROI, region of interest; SBRT, stereotactic body radiotherapy; SD, stable disease; SVM, support vector machine; TKI, tyrosine kinase inhibitor.

Received: January 19, 2022; Revised: September 27, 2022; Accepted: October 10, 2022.

## Introduction

Lung cancer is the second most frequently diagnosed cancer type and has the highest mortality in the world,<sup>1</sup> with non-small-cell lung cancer (NSCLC) accounting for 85% of all lung cancer cases.<sup>2</sup> In 2020, according to statistics from 185 countries, it was estimated that the number of diagnosed cases was approximately 2 206 771 (accounting for 11.4% of all cancers), and the number of deaths was 1 796 144 (18.0%),<sup>3</sup> with a 5-year relative survival rate of only 22%.<sup>4</sup> The high mortality rate of lung cancer is related to the high malignancy and late diagnosis of the tumor. More than 60% of lung cancer patients are in the locally advanced stage (stage III) or have metastases (stage IV) at the time of treatment initiation.<sup>5</sup> The 5-year relative survival rate in stage I patients is 57%, while that in stage IV patients drops to 4%.<sup>6</sup> Advanced patients urgently need precise and effective treatments to improve their prognosis.

Although concurrent or sequential chemotherapy with radiotherapy has been a conventional treatment plan for inoperable NSCLC,<sup>7</sup> radiotherapy and chemotherapy have not yet entered the era of precision medicine. In different patients, the sensitivity of tumor cells to treatment and the efficacy of radiotherapy are different.<sup>8</sup> Some patients experience no obvious benefit after receiving radiotherapy. The tumor may still progress locally or even metastasize to distant organs. Some patients may also suffer additional radiotherapy-related adverse reactions (radiation pneumonitis, radiation esophagitis, bone marrow suppression, etc) due to exposure of normal tissues to radiation, resulting in unnecessary burden of medical expenses. At present, response evaluation criteria in solid tumors (RECIST) standards are mostly used in clinics for efficacy evaluation<sup>9</sup>; this method compares and classifies the changes in tumor and lymph node diameters on computed tomography (CT) images before and after treatment. However, the response of NSCLC tumors to radiotherapy and chemotherapy may be slow,<sup>10</sup> resulting in a delay in the evaluation of efficacy. Furthermore, clinically, there is still a lack of early effective treatment sensitivity predictors to help clinicians evaluate the treatment response of the tumor before radiotherapy and adjust the treatment plan accordingly (such as enhanced chemotherapy or combined targeted or immunotherapy, etc) to improve patient prognosis.

Radiomics is an image analysis technique that enables quantitatively extracted image features from traditional medical images. Radiomics methods show strong predictive performance in the diagnosis and treatment of lung cancer. At present, radiomics methods have been employed to address various questions in the field of lung cancer, especially in NSCLC, including diagnosis

and identification,<sup>11,12</sup> staging, pathological typing,<sup>13</sup> degree of differentiation, genotyping,<sup>14,15</sup> selection of treatment options, toxic side effects,<sup>16</sup> and prognostic evaluation.<sup>17,18</sup> The process mainly includes data collection, image segmentation, feature extraction, feature selection, and model construction.<sup>19</sup> In the diagnosis and treatment of lung cancer patients, CT is the preferred imaging examination method, and it is also the most widely used method in radiomics research. As lung tumors present a strong contrast in CT images, including differences in gray value intensity, texture differences, and shape differences of tumors in the image, it can provide guidance for clinical diagnosis and treatment. However, there have only been a few studies on radiosensitivity of NSCLC using CT-based radiomics until now.<sup>20,21</sup> In previous studies using radiomics models to predict radiotherapy sensitivity, one study has explored the predictive performance of radiomics models and confirmed that they can accurately predict radiotherapy sensitivity.<sup>21</sup> However, that study lacked the discussion of clinical factors involved. A number of studies have confirmed that the combination of radiomic features (such as intensity, shape, texture, or wavelet) extracted from medical images with clinical parameters can make clinical decision-making more accurate.<sup>22</sup> Therefore, we aimed to develop and validate a prognostic model based on CT radiomics combined with clinical features to predict the radiotherapy sensitivity in patients with inoperable stage III and IV NSCLC.

## Materials and Methods

This study was conducted in accordance with the Declaration of Helsinki and approved by the Ethics Committee of Kunming Medical University in Yunnan Province (approval number: KYLX202175). Informed consent was waived by the committee because of the retrospective nature of this study. The reporting of this study conforms to the Strengthening the Reporting of Observational Studies in Epidemiology (STROBE) guidelines.<sup>23</sup> We have de-identified all patient details to ensure the confidentiality of patient information.

**Patients:** In this retrospective study, we selected patients with inoperable stage III and IV NSCLC at the Yunnan Cancer Hospital between October 2016 and September 2020. All patients received a complete standard radiotherapy regimen (60–66Gy/30–33f, intensity-modulated radiation therapy [IMRT] or 45–54Gy/5–10f, stereotactic body radiotherapy [SBRT]). Chemotherapy consists of two-drug cis/carboplatin-based regimens. Patients were treated with common chemotherapy regimens of cis/carboplatin plus etoposide or paclitaxel or pemetrexed every 21 days during radiotherapy. The platinum-partnered number of cycles depended

on the histology and response of the tumor. Clinical data including medical records, laboratory examinations, and CT chest scan findings were collected. The inclusion criteria were as follows: (1) pathological examination confirmed NSCLC; (2) clinical stage III and IV according to the Eighth Edition of the American Joint Committee on Cancer guidelines; (3) no indication for surgery; and (4) Karnofsky performance scale score  $\geq 70$  points. The exclusion criteria were: (1) incomplete medical records (such as unclear TNM stage, unknown specific time and dose records of radiotherapy, and incomplete laboratory examination data); (2) interruption of the radiotherapy process; (3) non-primary lung radiotherapy; (4) receiving other treatments besides chemotherapy before radiotherapy, such as targeted therapy or immunotherapy; and (5) incomplete or poor quality CT images (CT images were missing within 1 month before or within 3 months after radiotherapy; CT images with interference factors such as respiratory movement or metal artifacts that make the image unclear, etc).

Our main study endpoint was the patient's response to radiotherapy. According to the RECIST v1.1 evaluation standard,<sup>9</sup> the local response of the lesion was evaluated as complete response (CR), partial response (PR), stable disease (SD), and progressive disease (PD) by comparing CT images before and after radiotherapy. The radiation-sensitive group was defined as CR + PR, and the non-sensitive group was defined as SD + PD. Model predictive power was evaluated using the AUC.

Overall survival (OS) was defined as the time from the patient receiving radiotherapy to death due to any reason (for subjects who have been lost to follow-up before death, the time of the last medical record was calculated as the time of death).

**CT examination acquisition:** All images were obtained with a Siemens Somatom definition or Philips Brilliance, 64-slice, CT scanner. The imaging parameters were as follows: tube voltage, 90-120 kVp; automatic tube current modulation; collimation, 0.6 mm  $\times$  64; matrix, 512  $\times$  512; rotation time, 0.6 s, reconstruction slice thickness, 1 or 2 mm. Detailed CT scanning parameters are provided in Supplementary Table 1.

**The region of interest (ROI):** Two radiologists used ITK-SNAP software (version 3.8.0; <http://www.itksnap.org>) to manually delineate lung lesions at all levels in the soft tissue window and lung window CT images layer by layer.<sup>24</sup>

**Feature extraction:** We used the Analysis-kit software (AK, version 3.2.0, GE Healthcare) to extract the texture features of the lesion image from the above ROI, which is one of the commonly used software in radiomics feature extraction and can extract a series of common radiomic features.<sup>25</sup> To ensure a standardized voxel spacing in the entire queue, it was resampled to 0.8  $\times$  0.8  $\times$  1.5 mm<sup>3</sup> before feature extraction. The box width was set to 25 housefield units (HU). In total, 2460 radiomics features were extracted from the soft tissue window and lung window images. To eliminate the large differences in the original feature data of different radiomics, all features underwent maximum and minimum normalization processing<sup>26</sup> (the specific formula was:  $x' = (x - \min) / (\max - \min)$ ); where  $x'$  represents the value of a single data, min is the minimum value of the column where the data was

located, and max is the maximum value of the column where the data was located).

**Feature screening and model establishment:** We imported the radiomics features extracted above into FeAture Explorer (FAE, version 0.3.7; <https://github.com/salan668/FAE>) software based on Python (3.7.6).<sup>27</sup> To avoid group bias from differences in clinical characteristics, we randomly divided patients into training and testing sets at 7:3 according to the basic clinical characteristics of sex, age, smoking history, family history, pathology type, etc. Among them, the training set included 73 patients (28/45 = sensitive/non-sensitive) and 31 in the testing set (12/19 = sensitive/non-sensitive). To eliminate the imbalance between the training set data, we used UpSampling to randomly increase the number of samples to achieve a balance between the positive and negative samples. At the same time, two normalization methods (None normalization and MinMax normalization), one dimensionality reduction method (Pearson correlation coefficients), and four feature selectors (ANOVA, KW, Relief, and RFE) were used. The first 25 features and 10 categorizers (Adaboost, AE, Decision Tree, Gaussian Process, LDA, Logistic Regression, LR-Lasso, Naive Bayes, Random Forest, and SVM) were used for permutations to construct 2000 (2  $\times$  1  $\times$  4  $\times$  25  $\times$  10) models. Five-fold cross-validation was used on the training data set. For all constructed models, the receiver operating characteristic (ROC) curve analysis was used to evaluate the prediction performance, and the AUC was calculated for quantitative analysis. The critical value of the largest Youden's index was selected to calculate the accuracy, sensitivity, specificity, positive predictive value (PPV), and negative predictive value (NPV). After comparing the above parameters, the 16 features contained in the optimized model were selected. Due to the small number of samples and the large number of features, we further adopted the ANOVA and SVM for feature selection and model building based on these 16 features to prevent the model from over-fitting. Nine features were finally selected for modeling. The radiomics score (Rad-Score) was calculated based on the selected radiomics features and corresponding functional relationships.

**Selection of clinical features:** The clinical data of the patients (eg, age, sex, smoking history, family history, pathological type, clinical stage, and blood test results within 1 week before radiotherapy [platelet count, neutrophil ratio, monocyte ratio, lymphocyte ratio, and carcinoembryonic antigen (CEA) level], etc) were collected. Univariate regression analysis was performed on the clinical variables one by one. To avoid the interference of confounding factors leading to the omission of related features, the variables with  $P$  values less than 0.15 in univariate analyses were further analyzed by multivariate logistic regression to assess clinical factors significantly associated with radiosensitivity.<sup>28</sup>

**Combined model construction:** A combined model incorporating Rad-Score and clinical factors was built with the least absolute shrinkage and selection operator (LASSO) logistic regression. Then, the ROC curve analysis and calculation of the AUC value were conducted to evaluate the predictive performance of the combined model.

**Statistical analyses:** Continuous variables are represented using mean  $\pm$  standard deviation or median and quartile, and categorical

**Table 1.** Baseline Patient Characteristics.

	Total, n (%)	Training, n (%)	Testing, n (%)	P-value
Group				0.973
Non-sensitive	64 (61.5%)	45 (61.6%)	19 (61.3%)	
Radio-sensitive	40 (38.5%)	28 (38.4%)	12 (38.7%)	
Sex				0.063
Male	89 (85.6%)	66 (90.4%)	23 (74.2%)	
Female	15 (14.4%)	7 (9.6%)	8 (25.8%)	
Age (years)	57.35 ± 9.554	57.14 ± 9.375	57.84 ± 10.103	0.734
Pathology				0.377
Adenocarcinoma	37 (35.6%)	24 (32.9%)	13 (41.9%)	
Squamous cell carcinoma	67 (64.4%)	49 (67.1%)	18 (58.1%)	
Smoke				0.410
Yes	73 (70.2%)	53 (72.6%)	20 (64.5%)	
No	31 (29.8%)	20 (27.4%)	11 (35.5%)	
Family history				1.000
Yes	11 (10.6%)	8 (11.0%)	3 (9.7%)	
No	93 (89.4%)	65 (89.0%)	28 (90.3%)	
T stage				0.158
1	5 (4.8%)	4 (5.5%)	1 (3.2%)	
2	29 (27.9%)	18 (24.7%)	11 (35.5%)	
3	19 (18.3%)	11 (15.1%)	8 (25.8%)	
4	51 (49.0%)	40 (54.8%)	11 (35.5%)	
N stage				0.208
0	17 (16.3%)	13 (17.8%)	4 (12.9%)	
1	6 (5.8%)	3 (4.1%)	3 (9.7%)	
2	47 (45.2%)	37 (50.7%)	10 (32.3%)	
3	34 (32.7%)	20 (27.4%)	14 (45.2%)	
M stage				0.278
0	62 (59.6%)	46 (63.0%)	16 (51.6%)	
1	42 (40.4%)	27 (37.0%)	15 (48.4%)	
Stage				0.595
IIIA	24 (23.1%)	16 (21.9%)	8 (25.8%)	
IIIB	28 (26.9%)	22 (30.1%)	6 (19.4%)	
IIIC	10 (9.6%)	8 (11.0%)	2 (6.5%)	
IV	42 (40.4%)	27 (37.0%)	15 (48.4%)	
CCRT				0.477
Yes	35 (33.7%)	23 (31.5%)	12 (38.7%)	
No	69 (66.3%)	50 (68.5%)	19 (61.3%)	
NLR	1.885 (1.275, 2.698)	1.780 (1.260, 2.675)	2.060 (1.390, 3.010)	0.384
PLT_rank				0.665
Normal	91 (87.5%)	63 (86.3%)	28 (90.3%)	
Reduced	7 (6.7%)	7 (9.6%)	0	
Elevated	6 (5.8%)	3 (4.1%)	3 (9.7%)	
N_rank				0.559
Normal	96 (92.3%)	68 (93.2%)	28 (90.3%)	
Reduced	4 (3.8%)	4 (5.5%)	0	
Elevated	4 (3.8%)	1 (1.4%)	3 (9.7%)	
M_rank				0.129
Normal	81 (77.9%)	54 (74.0%)	27 (87.1%)	
Reduced	3 (2.9%)	2 (2.7%)	1 (3.2%)	
Elevated	20 (19.2%)	17 (23.3%)	3 (9.7%)	
L_rank				0.937
Normal	88 (84.6%)	62 (84.9%)	26 (83.9%)	
Reduced	14 (13.5%)	9 (12.3%)	5 (16.1%)	
Elevated	2 (1.9%)	2 (2.7%)	0	
CEA_rank				0.121
Normal	35 (33.7%)	28 (38.4%)	7 (22.6%)	
Elevated	69 (66.3%)	45 (61.6%)	24 (77.4%)	

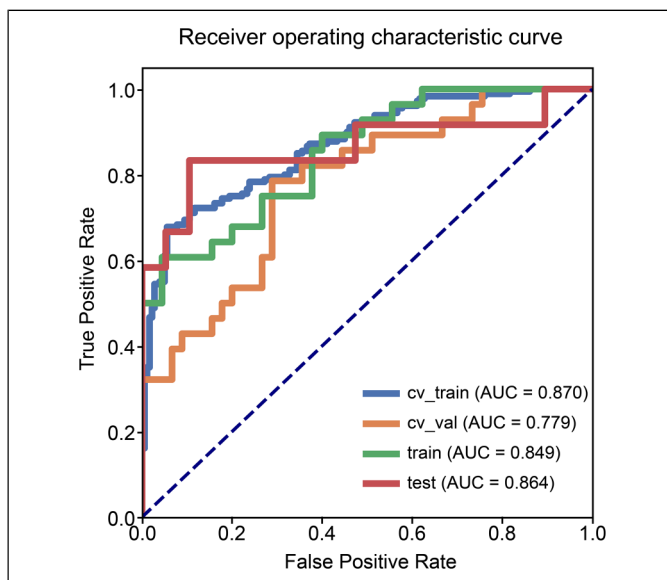
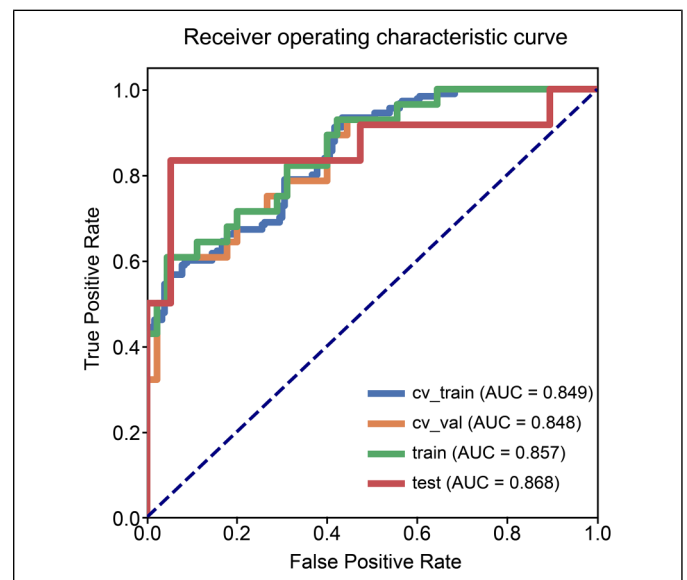
Abbreviations: CCRT, concurrent chemoradiotherapy; CEA, carcinoembryonic antigen; L, lymphocyte; M, monocyte; N, neutrophil; NLR, neutrophil-to-lymphocyte ratio; PLT, platelet.

**Table 2.** Statistics in the Prediction.

Statistics	Radiomics model			Combined model		
	Training set	Testing set	Cross-validation set	Training set	Testing set	Cross-validation set
ACC	0.822	0.871	0.740	0.822	0.903	0.822
AUC (95% CIs)	0.849 (0.755-0.931)	0.864 (0.683-0.996)	0.779 (0.655-0.878)	0.857 (0.761-0.935)	0.868 (0.689-1.000)	0.848 (0.735-0.930)
NPV	0.796	0.895	0.842	0.796	0.900	0.796
PPV	0.895	0.833	0.629	0.895	0.909	0.895
SEN	0.607	0.833	0.786	0.607	0.833	0.607
SPE	0.956	0.895	0.711	0.956	0.947	0.956

Data in parentheses are 95% CIs.

Abbreviations: ACC, accuracy; AUC, area under the curve; CI, confidence interval; NPV, negative predictive value; PPV, positive predictive value; SEN, sensitivity; SPE, specificity.

**Figure 1.** Receiver operating characteristic curves of the radiomics model.**Figure 2.** Receiver operating characteristic curves of the combined model.

variables are represented as frequency and percentage. The independent sample Student's t-test was used for continuous variables, categorical variables were analyzed using chi-square or Fisher's exact tests, and Wilcoxon rank-sum tests were performed for ranked data.  $P < 0.05$  was considered statistically significant. Survival curves were generated using the Kaplan–Meier Method. All statistical analyses were performed using SPSS (version 26.0) and R software (version 4.1.2; <https://www.R-project.org>).

## Results

### Baseline Characteristics

A total of 104 patients with NSCLC were included in this study. The clinical information of the patients is shown in Table 1. The overall average age was  $57.35 \pm 9.554$  (range: 31–80) years old, including 89 males (85.6%) and 15 females (14.4%). There were 67 cases (64.4%) of squamous

cell carcinoma and 37 cases (35.6%) of adenocarcinoma. More than 70% of patients had a history of smoking. Among them, those in the training set and the test set had no significant differences in clinical baseline characteristics (sex, age, pathological type, smoking history, family history, clinical stage, etc) (Table 1).

### Radiomics Features

A total of 2460 radiomic features (1228 and 1232 from lung and mediastinal windows, respectively) were extracted from the ROI of each lesion, including first-order features, shape features, and textural features (such as gray-level co-occurrence matrix [GLCM], gray-level size zone matrix [GLSZM], gray-level run length matrix [GLRLM], neighboring gray tone difference matrix [NGTDM], and gray-level dependence matrix [GLDM]).

The performance of the radiomics model based on the 9 radiomics features for predicting radiosensitivity is shown in Table 2.

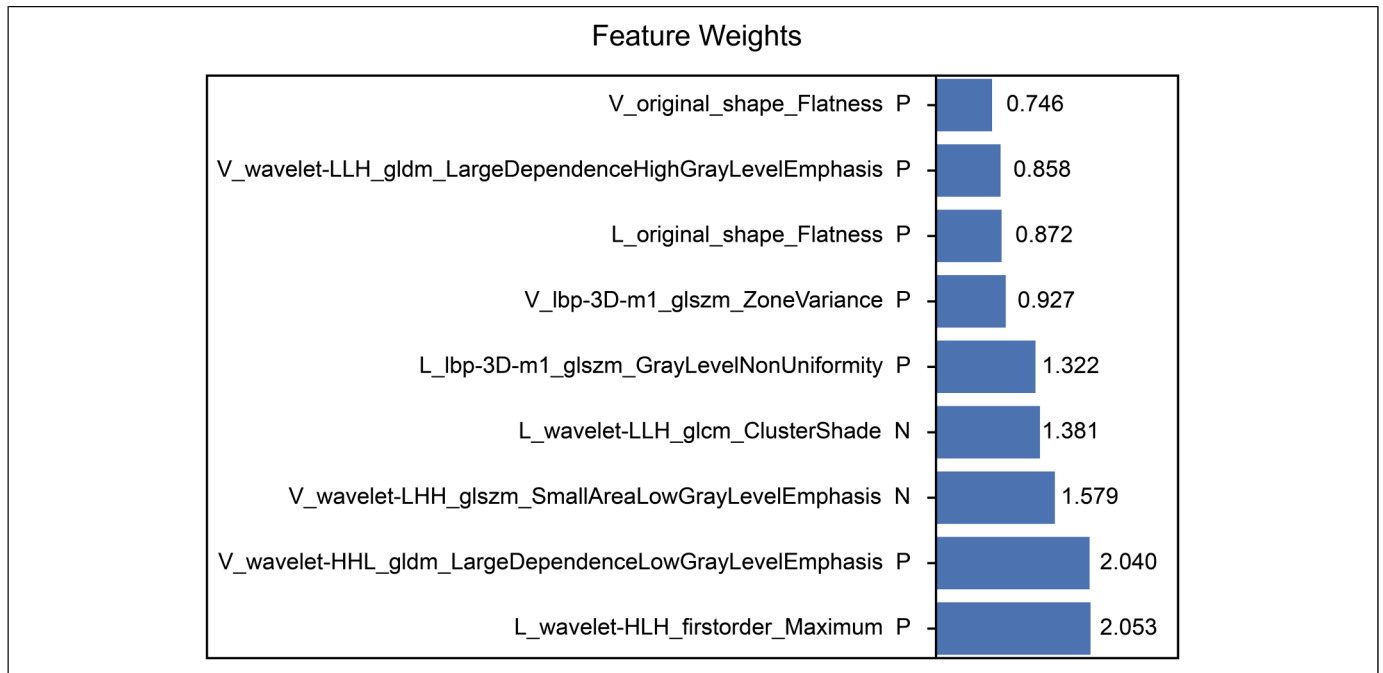


**Figure 3.** Nine features selected are presented. The coefficient indicates the feature's contribution to the model.

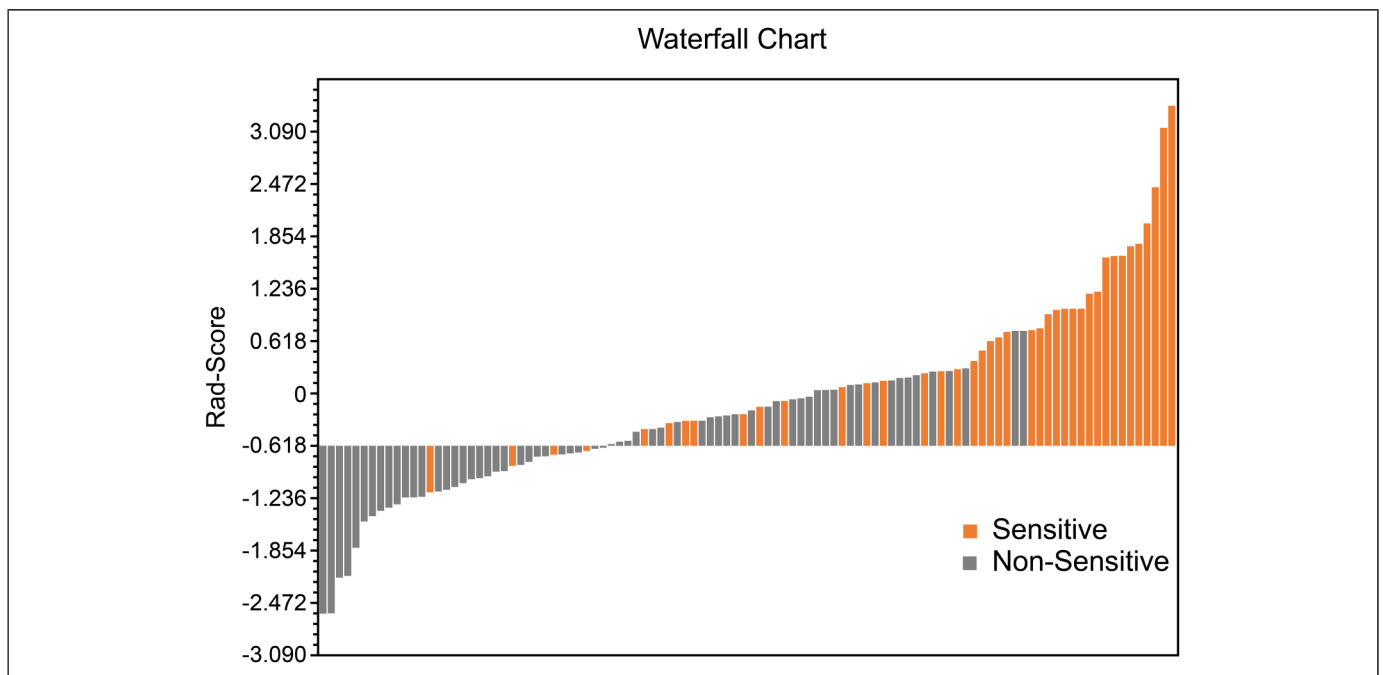


**Figure 4.** Waterfall chart reflects the performance of the Rad-Score in the prediction of radiotherapy sensitivity.

The accuracy of the model in the training, testing, and cross-validation sets was 0.822, 0.871, and 0.740, respectively, and the AUC values were 0.849 (95% confidence interval [CI]: 0.755-0.931), 0.864 (95% CI: 0.683-0.996), and 0.779 (95% CI: 0.655-0.878), respectively. The corresponding ROC curves are shown in Figure 1. The Rad-Score was calculated based on the selected features and their coefficients (Supplemental

Appendix A: Rad-Score, Figure 3), and the waterfall chart reflects the performance of the Rad-Score in the prediction (Figure 4).

### Clinical Features

In the univariate analysis of clinical baseline characteristics, we identified several clinical characteristics related to

**Table 3.** Univariate and Multivariate Analyses of Factors Associated with Radiotherapy Sensitivity.

Clinical factors	Univariate logistic regression		Multivariate logistic regression	
	OR (95% CIs)	<i>P</i> -value	OR (95% CIs)	<i>P</i> -value
Sex	Reference	0.199		
Male	4.154 (0.473, 36.494)			
Female				
Age	1.005 (0.955, 1.057)	0.853		
Pathology	Reference		Reference	
Adenocarcinoma	1.379 (0.496, 3.833)	0.537	1.277 (0.329, 4.951)	0.723
Squamous cell carcinoma				
Smoke	Reference	0.055	Reference	0.089
No				
Yes	3.310 (0.975, 11.234)		3.281 (0.833, 12.916)	
Family history	Reference	0.477		
No				
Yes	1.708 (0.391, 7.464)			
Stage	Reference	0.234	Reference	0.491
IIIA				
IIIB	0.444 (0.119, 1.656)	0.227	0.501 (0.119, 2.111)	0.346
IIIC	0.778 (0.142, 4.265)	0.772	1.077 (0.173, 6.699)	0.937
IV	0.272 (0.073, 1.009)	0.052	0.364 (0.074, 1.797)	0.215
CCRT	Reference	0.103	Reference	0.048
No				
Yes	2.318 (0.843, 6.372)		3.282 (1.010, 10.663)	
NLR	1.281 (0.854, 1.922)	0.231		
PLT_rank	Reference	0.552		
Normal				
Reduced	0.650 (0.117, 3.619)	0.623		
Elevated	3.250 (0.279, 37.803)	0.346		
N_rank	Reference	0.897		
Normal				
Reduced	1.615 (0.214, 12.178)	0.642		
Elevated	0.000	1.000		
M_rank	Reference	0.667		
Normal				
Reduced	1.455 (0.086, 24.512)	0.795		
Elevated	0.606 (0.187, 1.965)	0.404		
L_rank	Reference	0.186	Reference	0.201
Normal				
Reduced	3.905 (0.887, 17.194)	0.072	4.116 (0.814, 20.824)	0.087
Elevated	1.952 (0.116, 32.796)	0.642	3.080 (0.120, 79.145)	0.497
CEA_rank	Reference	0.178		
Normal				
Elevated	2.000 (0.729, 5.485)			

Data in parentheses are 95% CIs.

Abbreviations: CCRT, concurrent chemoradiotherapy; CEA, carcinoembryonic antigen; CI, confidence interval; L, lymphocyte; M, monocyte; N, neutrophil; NLR, neutrophil-to-lymphocyte ratio; OR, odds ratio; PLT, platelet.

radiotherapy sensitivity: smoking history, clinical stage, concurrent chemoradiotherapy (CCRT), and lymphocyte level status. Among the clinical characteristics, the *P*-value of the pathological type was greater than 0.15. However, in the actual theory, different types of cells had different responses to treatment; therefore, the pathological types were included in the multivariate logistic regression for analysis. In the multivariate analysis, only the clinical factor of CCRT showed significant differences between the radiation-sensitive and non-sensitive groups (Table 3).

### Combined Model

As shown in Figure 2 and Table 2, the combined model based on Rad-Score and CCRT had higher AUC values in the training (AUC = 0.857; 95% CI, 0.761-0.935), testing (AUC = 0.868; 95% CI, 0.689-1.000), and cross-validation sets (AUC = 0.848, 95% CI, 0.735-0.930). The accuracy of the testing set and cross-validation set increased to 0.903 and 0.822, respectively (Table 2). In addition, the sensitivity of the cross-validation set of the combined model was reduced compared with the radiomics model, but the specificity of the testing set

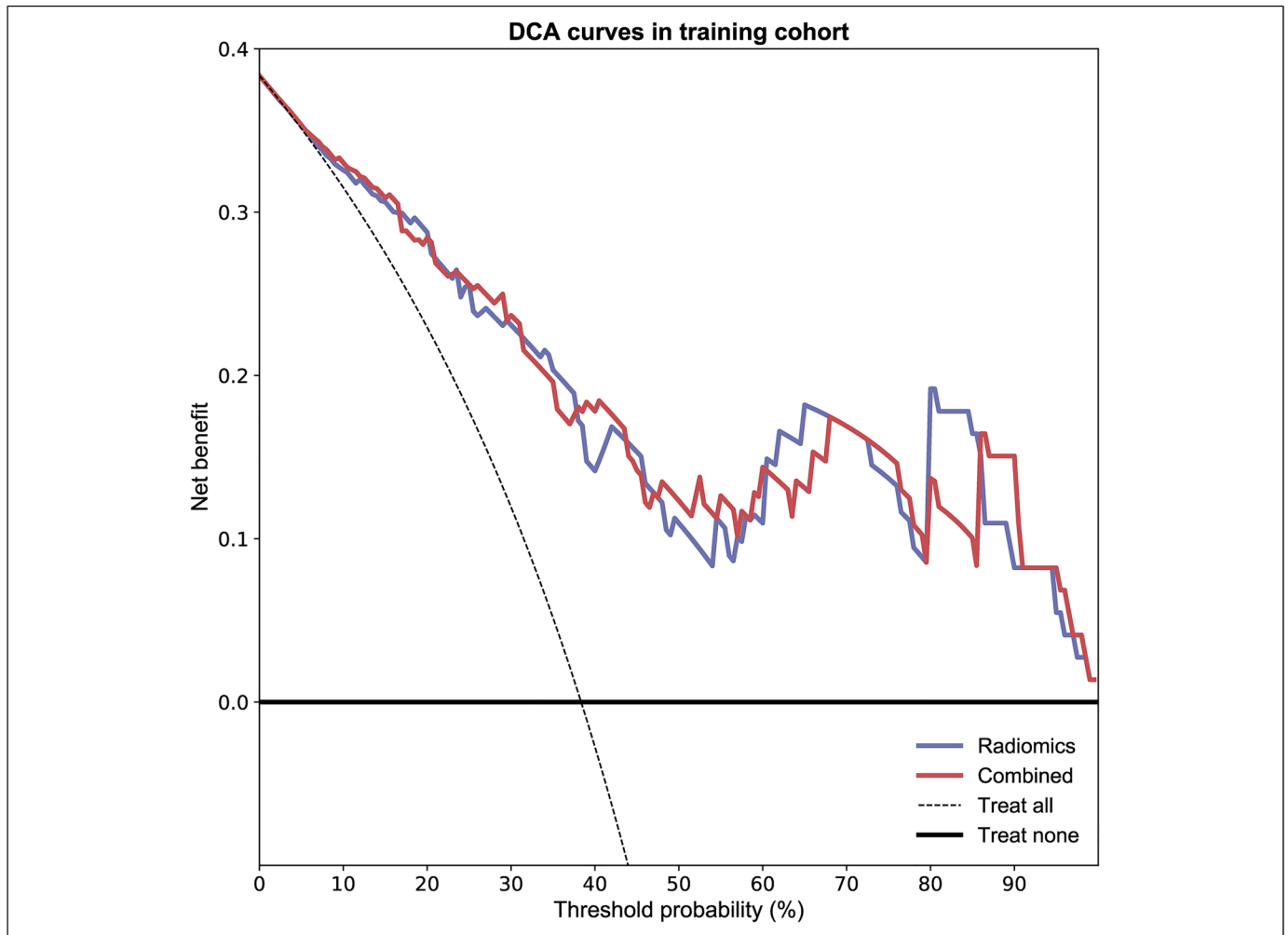


**Figure 5.** The decision curve analyses of the radiomic model and combined model in the training cohort.

and the cross-validation set was improved. The calibration plot revealed good predictive accuracy between the actual probability and prediction probability (Supplementary Figure 1). Decision curve analysis (DCA) further demonstrated higher overall net benefit for the combined model compared with the radiomic model (Figures 5 to 7).

### Survival Analysis Related with Each Factor

In the entire cohort, the median follow-up was 17.0 months (range: 2.0-52.0 months). Univariate and multivariate Cox regression analyses showed that neither concurrent chemotherapy nor Rad-Score had a significant correlation with OS. Univariate analysis revealed that platelet level status was significantly associated with OS ( $\chi^2 = 7.095$ ,  $P = 0.029$ ). The median survival times in the patients with reduced, normal, and elevated platelet levels were 15.0 months (95% CI: 0.000-30.397), 18.0 months (95% CI: 15.251-20.749), and 6.0 months (95% CI: 0.000-21.603), respectively (Figure 8).

### Discussion

In this study, the radiomics model we established performed well in predicting radiosensitivity in patients with inoperable stage III and IV NSCLC. This result proves that radiomics features have a certain role in predicting the short-term response to radiotherapy in NSCLC. We screened nine features in the radiomics model, and their meanings are explained in the appendix, respectively. Among the selected radiomics features, *L\_wavelet-HLH\_firstorder\_Maximum*, *V\_wavelet-HHL\_gldm\_LargeDependenceLowGrayLevelEmphasis*, and *V\_wavelet-LHH\_glszm\_SmallAreaLowGrayLevelEmphasis* have a higher weight in the radiomics score, indicating that the greater the maximum gray level intensity, the rougher the texture of the tumor, and the better the radiotherapy sensitivity. At the same time, we found that concurrent chemoradiotherapy is also associated with radiosensitivity, and the combined model based on radiomics scores and clinical factors not only improved AUC values, but also demonstrated a higher overall net benefit.

In view of the analysis of clinical factors in this study, CCRT can improve the treatment response to radiotherapy in patients



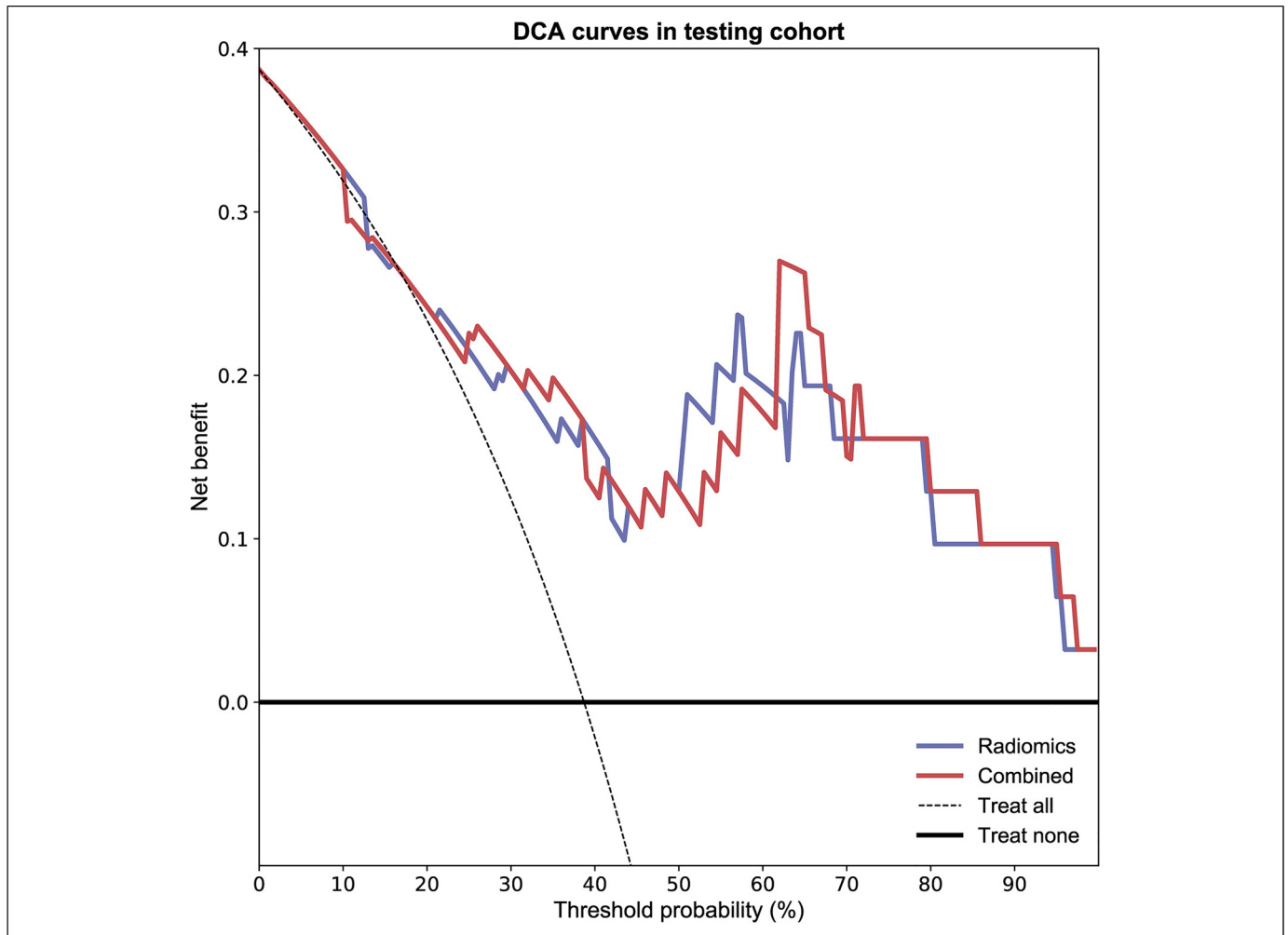


**Figure 6.** The decision curve analyses of the radiomic model and combined model in the testing cohort.

with NSCLC. However, not all patients can tolerate the toxic side effects caused by concurrent radiotherapy and chemotherapy in the clinical treatment process. As a result, patients with poor radiotherapy sensitivity may accept combination therapy, such as combined immunotherapy or targeted therapy, to improve radiation therapy efficiency if they cannot tolerate chemotherapy-related side effects.<sup>29</sup> Among these, the optimized combination of radiotherapy and immunotherapy is an emerging field. Studies have shown that radiotherapy may stimulate or enhance the response to immune checkpoint inhibitors.<sup>30</sup> The combination of immune checkpoint inhibitors and local radiotherapy will improve the control of local and distant metastases and ultimately improve the clinical outcome of patients with oligometastatic cancer.<sup>31</sup> Therefore, the combination of radiotherapy and immunotherapy has certain prospects. Of course, this requires more experimental research to further explore this aspect and validate the effectiveness of this approach. In addition, the advancement of targeted therapy research, especially the development of tyrosine kinase inhibitors (TKIs), has also had a positive impact on therapeutic approaches. Studies have shown that the response to

radiotherapy varies depending on the molecular status of tumors, and *EGFR*-mutated tumors respond well to radiotherapy.<sup>32</sup> Another study on early lung adenocarcinoma found that *KRAS* mutations were associated with poor local control of SBRT treatment.<sup>33</sup> Studies have also shown that the first-line use of radiotherapy and TKI treatment patterns are associated with better prognosis,<sup>34</sup> while the use of upfront epidermal growth factor receptor-TKI (EGFR-TKI), and deferral of radiotherapy, is associated with inferior OS in patients with *EGFR*-mutant NSCLC who develop brain metastases.<sup>35</sup> Precise lung cancer treatment includes not only precise radiotherapy technology but also precise targeted and immunotherapy. All of the above will be used to direct further research in the future and to provide help for each patient in choosing a more personalized treatment plan.

In our study, synchronized chemotherapy apparently did not help with survival. This result is quite different from that of many previous studies and meta-analyses in which concurrent chemotherapy improves OS; we believe that a possible reason is that most of the patients in this study had advanced T stage (about 67% of patients with T3-4). For these patients with

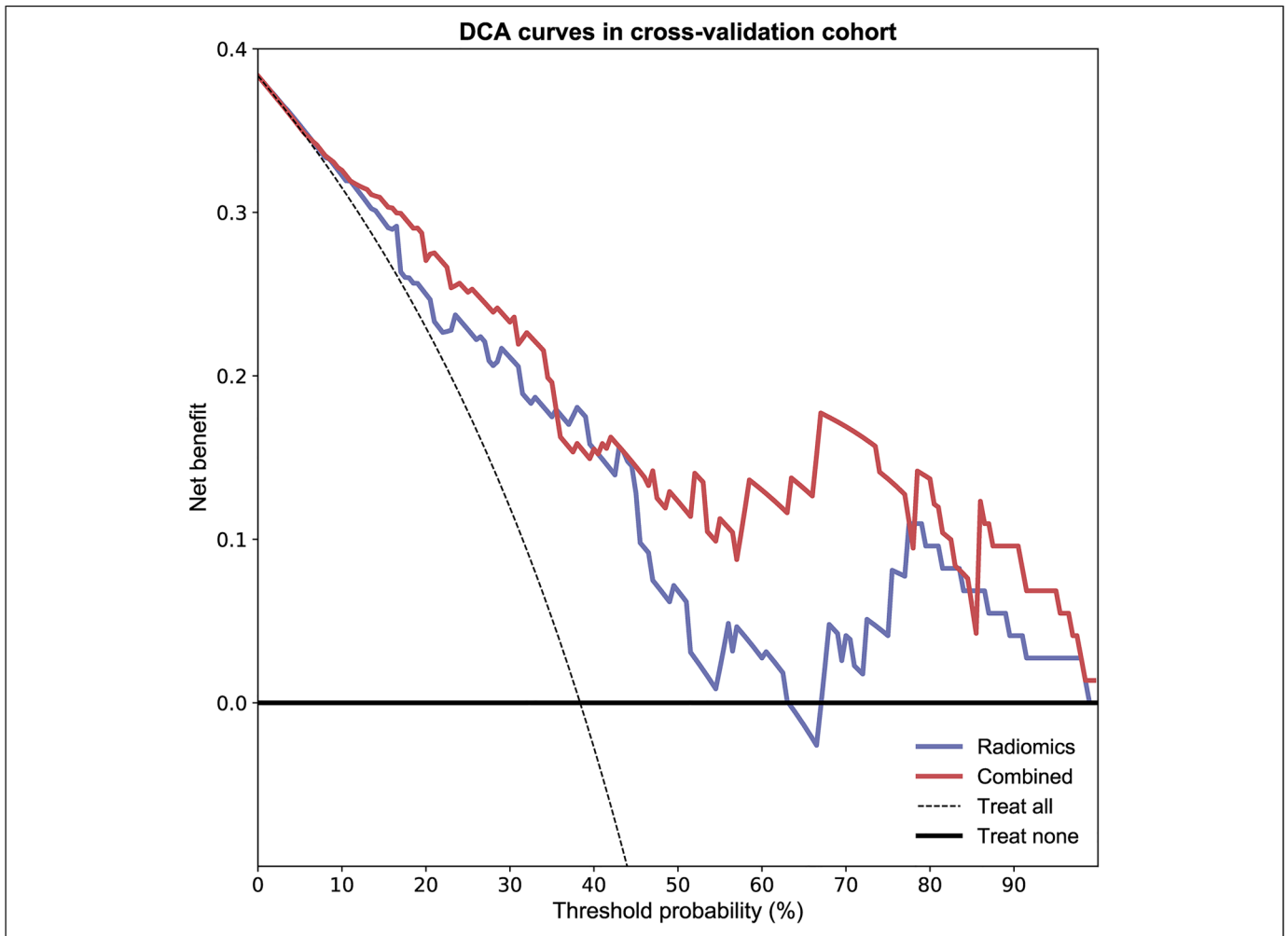


**Figure 7.** The decision curve analyses of the radiomic model and combined model in the cross-validation cohort.

large tumor volumes and extensive invasion of adjacent tissues and organs (such as the heart, esophagus, large blood vessels, etc.), local treatment is more difficult, increasing the radiation dose cannot preserve important tissues and organs, and reducing the radiation dose cannot achieve radical tumor cure. It is also more difficult to set up a field in the target area of radiotherapy. Therefore, most patients received several cycles of induction chemotherapy before radiotherapy to reduce the tumor treatment volume and normal tissue damage caused by radiotherapy. This is different from the rigorous CCRT in previous studies. Moreover, the results obtained in this study that CCRT after induction chemotherapy did not increase the survival benefit were consistent with the results of previous studies. Ardizzoni found that the addition of single agent taxane given concurrently to radiotherapy failed to significantly improve survival after platinum-based induction in locally advanced NSCLC.<sup>36</sup>

In addition, a number of previous studies have discussed the role of the neutrophil-to-lymphocyte ratio (NLR) in the prognostic assessment of NSCLC and have demonstrated that an increase in NLR over the course of radiotherapy had

a negative impact on survival.<sup>37</sup> Some studies have shown that NLR is associated with inferior outcomes in localized NSCLC treated with SBRT.<sup>38</sup> In the results of this study, neither the univariate nor multivariate analysis showed a statistically significant impact of NLR. A possible reason is that some patients have received chemotherapy before radiotherapy, and the hematological toxicity of chemotherapy leads to different results of hematological examinations, which causes interference.

In the exploration of factors related to survival prognosis, we did not find a significant correlation between radiotherapy sensitivity and OS. There are several possible reasons worth considering for this observation. One reason for the failure to achieve significant survival-related benefits in patients with radiation-sensitive tumors is the limitation of radiotherapy associated with its side effects. Regarding this limitation, we need to consider whether an individualized dose setting in radiotherapy-sensitive patients is required, which, of course, requires further intensive investigation. In addition, in stage IV patients, death can be caused by metastases.

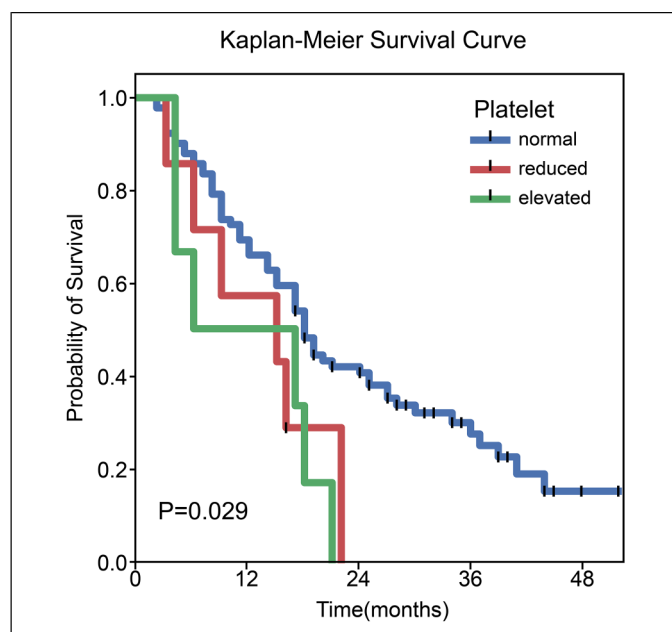


**Figure 8.** Kaplan–Meier curves of overall survival stratified by platelet levels ( $P = 0.029$ ).

We found that platelet level status was correlated with OS patients with NSCLC after radiotherapy. Patients with platelet levels higher than normal had a poor prognosis. A number of previous studies have confirmed the existence of thrombocytosis and platelet activation in cancer patients, which can promote the growth, invasion, metastasis, and other malignant behaviors of tumors through a variety of mechanisms<sup>39–41</sup> and are closely related to low survival rates. Our research results are consistent with these previous conclusions.

This study also had some limitations: (1) This was a single-center study with a small sample size. (2) The data collection was retrospective, and there may have been deviations in the record of previous medical records. (3) The study excluded patients who have received targeted or immunotherapy before radiotherapy, and there was a lack of research on these two types of patients. (4) The study included patients with NSCLC with different tumor node metastasis stages and failed to conduct a stratified analysis of the different stages.

## Conclusions

Radiomic features extracted from CT images combined with clinical features have potential value in predicting radiosensitivity, which may provide more accurate treatment strategy guidance for clinicians treating NSCLC. For radiation-insensitive patients, radiotherapists around the world are actively exploring further possibilities for locally advanced or metastatic cancer treatment to provide a greater advantage to bring more treatment benefits to patients.

## Acknowledgments

We would like to thank Editage ([www.editage.com](http://www.editage.com)) for English language editing and thank all colleagues involved in the study for their contributions.

## Declaration of Conflicting Interests

The author(s) declared no potential conflicts of interest with respect to the research, authorship, and/or publication of this article.

## Ethics Statement

This study was conducted in accordance with the Declaration of Helsinki and approved by the Ethics Committee of Kunming Medical University in Yunnan Province (approval number: KYLX202175). Informed consent was waived by the committee because of the retrospective nature of this study. We have de-identified all patient details to ensure the confidentiality of patient information.

## Funding

The author(s) disclosed receipt of the following financial support for the research, authorship, and/or publication of this article: This study was funded by the National Natural Science Foundation of China (No. 82060558), Yunnan Fundamental Research Projects (No. 202001AS70011), Ten-thousand Talents Program of Yunnan Province (Yunling scholar), Yunnan Provincial Training Special Funds for High-level Health Technical Personnel (No. L-2018001), Yunnan Health Training Project of High Level Talents (No. H-2019074), Kunming Medical University 2021 postgraduate innovation fund project (2021S254).

## ORCID iD

Wenhui Li  <https://orcid.org/0000-0002-0312-7993>

## Supplemental Material

Supplemental material for this article is available online.

## References

- GBD 2019 Diseases and Injuries Collaborators. Global burden of 369 diseases and injuries in 204 countries and territories, 1990–2019: a systematic analysis for the global burden of disease study 2019. *Lancet*. 2020;396(10258):1204–1222. doi: 10.1016/S0140-6736(20)30925-9
- Molina JR, Yang P, Cassivi SD, Schild SE, Adjei AA. Non-small cell lung cancer: epidemiology, risk factors, treatment, and survivorship. *Mayo Clin Proc*. 2008;83(5):584–594. doi: 10.4065/83.5.584
- Sung H, Ferlay J, Siegel RL, et al. Global cancer statistics 2020: GLOBOCAN estimates of incidence and mortality worldwide for 36 cancers in 185 countries. *CA Cancer J Clin*. 2021;71(3):209–249. doi: 10.3322/caac.21660
- Siegel RL, Miller KD, Fuchs HE, Jemal A. Cancer statistics, 2022. *CA Cancer J Clin*. 2022;72(1):7–33. doi: 10.3322/caac.21708
- Meza R, Meernik C, Jeon J, Cote ML. Lung cancer incidence trends by gender, race and histology in the United States, 1973–2010. *PLoS One*. 2015;10(3):e0121323. doi: 10.1371/journal.pone.0121323

6. Miller KD, Nogueira L, Mariotto AB, et al. Cancer treatment and survivorship statistics, 2019. *CA Cancer J Clin.* 2019;69(5):363-385. doi: 10.3322/caac.21565
7. Maconachie R, Mercer T, Navani N, McVeigh G. Guideline committee. Lung cancer: diagnosis and management: summary of updated NICE guidance. *Br Med J.* 2019;364:l1049. doi: 10.1136/bmj.l1049
8. Zhivotovsky B, Joseph B, Orrenius S. Tumor radiosensitivity and apoptosis. *Exp Cell Res.* 1999;248(1):10-17. doi: 10.1006/excr.1999.4452
9. Eisenhauer EA, Therasse P, Bogaerts J, et al. New response evaluation criteria in solid tumours: revised RECIST guideline (version 1.1). *Eur J Cancer.* 2009;45(2):228-247. doi: 10.1016/j.ejca.2008.10.026
10. Werner-Wasik M, Xiao Y, Pequignot E, Curran WJ, Hauck W. Assessment of lung cancer response after nonoperative therapy: tumor diameter, bidimensional product, and volume. A serial CT scan-based study. *Int J Radiat Oncol Biol Phys.* 2001;51(1):56-61. doi: 10.1016/s0360-3016(01)01615-7
11. Wang Z, Li N, Zheng F, et al. Optimizing the timing of diagnostic testing after positive findings in lung cancer screening: a proof of concept radiomics study. *J Transl Med.* 2021;19(1):191. doi: 10.1186/s12967-021-02849-8
12. Chen BT, Chen Z, Ye N, et al. Differentiating peripherally-located small cell lung cancer from non-small cell lung cancer using a CT radiomic approach. *Front Oncol.* 2020;10:593. doi: 10.3389/fonc.2020.00593
13. Zhu X, Dong D, Chen Z, et al. Radiomic signature as a diagnostic factor for histologic subtype classification of non-small cell lung cancer. *Eur Radiol.* 2018;28(7):2772-2778. doi: 10.1007/s00330-017-5221-1
14. Rios Velazquez ER, Parmar C, Liu Y, et al. Somatic mutations drive distinct imaging phenotypes in lung cancer. *Cancer Res.* 2017;77(14):3922-3930. doi: 10.1158/0008-5472.CAN-17-0122
15. Liu G, Xu Z, Ge Y, et al. 3D Radiomics predicts EGFR mutation, exon-19 deletion and exon-21 L858R mutation in lung adenocarcinoma. *Transl Lung Cancer Res.* 2020;9(4):1212-1224. doi: 10.21037/tlcr-20-122
16. Yang P, Peng X, Jin H, et al. Radiological prediction model of lung radiation pneumonitis based on dose line segmentation. *Int J Radiat Oncol Biol Phys.* 2021;111(3):e459-e460. doi: 10.1016/j.ijrobp.2021.07.1289
17. Khorrami M, Prasanna P, Gupta A, et al. Changes in CT radiomic features associated with lymphocyte distribution predict overall survival and response to immunotherapy in non-small cell lung cancer. *Cancer Immunol Res.* 2020;8(1):108-119. doi: 10.1158/2326-6066.CIR-19-0476
18. Fave X, Zhang L, Yang J, et al. Delta-radiomics features for the prediction of patient outcomes in non-small cell lung cancer. *Sci Rep.* 2017;7(1):588. doi: 10.1038/s41598-017-00665-z
19. Gillies RJ, Kinahan PE, Hricak HH. Radiomics: images are more than pictures, they are data. *Radiology.* 2016;278(2):563-577. doi: 10.1148/radiol.2015151169
20. Chetan MR, Gleeson FV. Radiomics in predicting treatment response in non-small-cell lung cancer: current status, challenges and future perspectives. *Eur Radiol.* 2021;31(2):1049-1058. doi: 10.1007/s00330-020-07141-9
21. Yan M, Wang W. Radiomic analysis of CT predicts tumor response in human lung cancer with radiotherapy. *J Digit Imaging.* 2020;33(6):1401-1403. doi: 10.1007/s10278-020-00385-3
22. Krafft SP, Rao A, Stingo F, et al. The utility of quantitative CT radiomics features for improved prediction of radiation pneumonitis. *Med Phys.* 2018;45(11):5317-5324. doi: 10.1002/mp.13150
23. Von Elm E, Altman DG, Egger M, et al. The strengthening the reporting of observational studies in epidemiology (STROBE) statement: guidelines for reporting observational studies. *Ann Intern Med.* 2007;147(8):573-577. doi: 10.7326/0003-4819-147-8-200710160-00010
24. Yushkevich PA, Piven J, Hazlett HC, et al. User-guided 3D active contour segmentation of anatomical structures: significantly improved efficiency and reliability. *Neuroimage.* 2006;31(3):1116-1128. doi: 10.1016/j.neuroimage.2006.01.015
25. Li H, Zhu M, Jian L, et al. Radiomic score as a potential imaging biomarker for predicting survival in patients with cervical cancer. *Front Oncol.* 2021;11:706043. doi:10.3389/fonc.2021.706043
26. Haga A, Takahashi W, Aoki S, et al. Standardization of imaging features for radiomics analysis. *J Med Invest.* 2019;66(1):35-37. doi: 10.2152/jmi.66.35
27. Song Y, Zhang J, Zhang YD, et al. Feature explorer (FAE): a tool for developing and comparing radiomics models. *PLoS One.* 2020;15(8):e0237587. doi: 10.1371/journal.pone.0237587
28. Zhou ZR, Wang WW, Li Y, et al. In-depth mining of clinical data: The construction of clinical prediction model with R. *Ann Transl Med.* 2019;7(23):796. doi: 10.21037/atm.2019.08.63
29. Altorki NK, McGraw TE, Boreczuk AC, et al. Neoadjuvant durvalumab with or without stereotactic body radiotherapy in patients with early-stage non-small-cell lung cancer: a single-centre, randomised phase 2 trial. *Lancet Oncol.* 2021;22(6):824-835. doi: 10.1016/S1470-2045(21)00149-2
30. Sindoni A, Minutoli F, Ascenti G, Pergolizzi S. Combination of immune checkpoint inhibitors and radiotherapy: review of the literature. *Crit Rev Oncol Hematol.* 2017;113:63-70. doi: 10.1016/j.critrevonc.2017.03.003
31. Pitroda SP, Chmura SJ, Weichselbaum RR. Integration of radiotherapy and immunotherapy for treatment of oligometastases. *Lancet Oncol.* 2019;20(8):e434-e442. doi: 10.1016/S1470-2045(19)30157-3
32. Arrieta O, Ramírez-Tirado LA, Caballé-Perez E, et al. Response rate of patients with baseline brain metastases from recently diagnosed non-small cell lung cancer receiving radiotherapy according to EGFR, ALK and KRAS mutation status. *Thorac Cancer.* 2020;11(4):1026-1037. doi: 10.1111/1759-7714.13359
33. Cassidy RJ, Zhang X, Patel PR, et al. Next-generation sequencing and clinical outcomes of patients with lung adenocarcinoma treated with stereotactic body radiotherapy. *Cancer.* 2017;123(19):3681-3690. doi: 10.1002/cncr.30794
34. Wang X, Bai YF, Zeng M. First-line tyrosine kinase inhibitor with or without aggressive upfront local radiation therapy in patients with EGFRm oligometastatic non-small-cell lung cancer: interim results of a randomized phase III, open-label clinical trial (SINDAS) (NCT02893332). *Int J Radiat Oncol Biol Phys.* 2020;108(3):e81. doi: 10.1016/j.ijrobp.2020.07.1169

35. Magnuson WJ, Lester-Coll NH, Wu AJ, et al. Management of brain metastases in tyrosine kinase inhibitor-naïve epidermal growth factor receptor-mutant non-small-cell lung cancer: a retrospective multi-institutional analysis. *J Clin Oncol.* 2017;35(10):1070-1077. doi: 10.1200/JCO.2016.69.7144
36. Ardizzoni A, Tiseo M, Boni L, et al. Randomized phase III PITCAP trial and meta-analysis of induction chemotherapy followed by thoracic irradiation with or without concurrent taxane-based chemotherapy in locally advanced NSCLC. *Lung Cancer.* 2016;100:30-37. doi: 10.1016/j.lungcan.2016.07.026
37. Wang Z, Zhan P, Lv Y, et al. Prognostic role of pretreatment neutrophil-to-lymphocyte ratio in non-small cell lung cancer patients treated with systemic therapy: a meta-analysis. *Transl Lung Cancer Res.* 2019;8(3):214-226. doi: 10.21037/tlcr.2019.06.10
38. Sebastian N, Wu T, Bazan J, et al. Pre-treatment neutrophil-lymphocyte ratio is associated with overall mortality in localized non-small cell lung cancer treated with stereotactic body radiotherapy. *Radiother Oncol.* 2019;134:151-157. doi: 10.1016/j.radonc.2019.01.032
39. Falanga A, Russo L, Milesi V. The coagulopathy of cancer. *Curr Opin Hematol.* 2014;21(5):423-429. doi: 10.1097/MOH.0000000000000072
40. Gay LJ, Felding-Habermann B. Contribution of platelets to tumour metastasis. *Nat Rev Cancer.* 2011;11(2):123-134. doi: 10.1038/nrc3004
41. Schlesinger M. Role of platelets and platelet receptors in cancer metastasis. *J Hematol Oncol.* 2018;11(1):125. doi: 10.1186/s13045-018-0669-2